

Symmetric-Asymmetric transition in mixtures of Bose-Einstein condensates

Anatoly A. Svidzinsky and Siu-Tat Chui
Bartol Research Institute, University of Delaware, Newark, DE 19716
(November 29, 2018)

We propose a new kind of quantum phase transition in phase separated mixtures of Bose-Einstein condensates. In this transition, the distribution of the two components changes from a symmetric to an asymmetric shape. We discuss the nature of the phase transition, the role of interface tension and the phase diagram. The symmetric to asymmetric transition is the simplest quantum phase transition that one can imagine. Careful study of this problem should provide us new insight into this burgeoning field of discovery.

There is much recent interest in quantum phase transitions. Examples of these include the Wigner electron solid melting transition, the Mott-Hubbard metal-insulator transition, and different magnetic transitions. In physical phenomena involving Bose-Einstein condensates (BECs) quantum mechanics play a crucial role. In this paper we propose a new kind of quantum phase transitions in phase-separated mixtures of BEC condensates. In this transition, the distribution of the two components changes from a symmetric to an asymmetric shape. To explore this transition, we first investigate the stability of the symmetric phase by studying its normal modes. We find interface modes that become soft. When the lowest frequency becomes zero, the instability sets in and this determines the stability limit of the symmetric phase. We determine the actual phase boundary by comparing the energy between the symmetric phase and the asymmetric phase and find that this actual phase boundary and the instability boundary is not the same. This suggests that the transition is first order. The system may be a good laboratory to study issues of quantum metastability and tunnelling. The symmetric to asymmetric transition is the simplest quantum phase transition that one can imagine. Careful study of this problem should provide us new insight into this burgeoning field of discovery. We now describe the results in detail.

Mixtures of trapped Bose-Einstein condensates have recently received considerable theoretical [1,2,3,4,5,6,7] and experimental [8,9,10] interest. Experimentally at low fields, the spin exchange process can occur in an optically trapped condensate, leading to spin domains [10] with metastable behavior [11,12]. Binary condensates in two hyperfine levels of ^{87}Rb have been created and studied [8,13], most notably realizing a system of interpenetrating Bose fluids [9], measurements of phase dispersion [14], and a vortex state in a dilute-gas BEC [15].

The equilibrium density distributions of segregated mixtures in the absence of gravity have been studied numerically for different system parameters. Two types of configurations have been discussed: a symmetric [3,5,2] configuration, for which one component is inside the other one, and an asymmetric one in which the two components occupy the left and the right hand side of a sphere [5,2].

In general, the asymmetric phase possesses a lower interface energy. On the other hand, since the degree of self-repulsion may differ between the two species, the less self-repulsive component will prefer to remain where the density is higher, while the other component moves to the low density regions outside. This favors the symmetric phase. Depending on the system parameters, one of these two energetic considerations will win out. These system parameters can be adjusted by changing the trapping frequencies, the relative particle numbers of the two species, and the interaction between the particles with Feshbach resonances. We first address the stability of the symmetric phase.

We consider the two-component BEC in a spherically symmetric trap. The dynamics of this system is described by the time dependent Gross-Pitaevskii equations:

$$i\hbar \frac{\partial \Psi_1}{\partial t} = -\frac{\hbar^2}{2m} \Delta \Psi_1 + V_{\text{tr}} \Psi_1 + \frac{4\pi\hbar^2}{m} (a_{11} |\Psi_1|^2 + a_{12} |\Psi_2|^2) \Psi_1, \quad (1)$$

$$i\hbar \frac{\partial \Psi_2}{\partial t} = -\frac{\hbar^2}{2m} \Delta \Psi_2 + V_{\text{tr}} \Psi_2 + \frac{4\pi\hbar^2}{m} (a_{22} |\Psi_2|^2 + a_{12} |\Psi_1|^2) \Psi_2, \quad (2)$$

where $\Psi_{1,2}$ are the condensate wave functions, $V_{\text{tr}} = m\omega_0^2 r^2/2$ is the trapping potential, ω_0 is the trapping frequency, r is the radial spherical coordinate, $a_{ij} > 0$ are s -wave scattering lengths.

We shall assume in this paper that the condition $a_{12}^2 - a_{11}a_{22} > 0$ is satisfied and, therefore, the condensates are phase-segregated. We study the condensates in the TF limit. In this regime, the phase-segregated condensates

overlap over the length scale $\Lambda = \xi/\sqrt{a_{12}/\sqrt{a_{11}a_{22}} - 1}$, where ξ is the healing length [7]. For parameters of the JILA experiments on phase-segregated states $\Lambda \approx 47\xi$. If the penetration depth $\Lambda \ll R$, where R is the size of the system, the condensates can be approximately treated as nonoverlapping, which we assume to be the case. The effect of overlapping condensates results in a finite surface tension and can be included via boundary conditions at the interphase. If the condensates do not overlap one can neglect the last terms in Eqs. (1), (2). As a result, the dynamical equations for Ψ_1 and Ψ_2 decouple. However, the two condensates are coupled by the boundary conditions at the interface which require continuity of the pressure and the normal velocity.

The symmetric phase consists of a central core of the first component and an outer shell of the second species (we assume $a_{11} \leq a_{22}$). The stationary density distribution $n_i = |\Psi_i|^2$ of the two components is given by

$$G_{11}n_1 = \mu_1(1 - r^2/R_1^2), \quad 0 < r < R_*, \quad (3)$$

$$G_{22}n_2 = \mu_2(1 - r^2/R_2^2), \quad R_* < r < R_2, \quad (4)$$

where $G_{ii} = 4\pi\hbar^2 a_{ii}/m$, $R_i = \sqrt{2\mu_i/m\omega_0^2}$. The normalization condition $\int n_i dV = N_i$, where N_i are the numbers of condensate particles, determines the chemical potentials μ_i . The position of the phase boundary R_* is given by the condition that the pressures exerted by both condensates are equal $R_* = R_2\sqrt{(1 - \kappa\lambda)/(1 - \kappa)\lambda}$ [16], where we introduced the dimensionless parameters $\kappa = \sqrt{a_{11}/a_{22}}$, $\lambda = \mu_2/\mu_1$. The symmetric configuration is favorable when κ differs from unity, with the less repulsive component in the middle ($\kappa < 1$). At the interface between two components $n_2/n_1 = \kappa < 1$.

One can rewrite the time dependent Gross-Pitaevskii equations in a hydrodynamic form which shows an analogy between our problem and motion of two immiscible fluids. In the strong phase-segregated regime the dynamics of each component is described by the following Josephson hydrodynamic equations [17]

$$\frac{\partial n}{\partial t} + \nabla \cdot (n\mathbf{V}) = 0, \quad (5)$$

$$\frac{1}{2}mV^2 + V_{\text{tr}} - \frac{\hbar^2}{2m} \frac{1}{\sqrt{n}} \Delta \sqrt{n} + Gn + m \frac{\partial \Phi}{\partial t} = \mu, \quad (6)$$

where \mathbf{V} is the condensate velocity and Φ is the velocity potential, $\mathbf{V} = \nabla\Phi$. The trapping potential plays the role of gravitational potential in hydrodynamics. We look for small perturbation from the equilibrium state. The equation for perturbation in the velocity potential for each of the component is the same as the one component case [18]

$$\frac{2\omega^2}{\omega_0^2} \Phi - 2r \frac{\partial \Phi}{\partial r} + (R^2 - r^2) \Delta \Phi = 0. \quad (7)$$

Continuity of the pressure at the interphase results in the following boundary condition

$$\omega_0^2 R_* \frac{\partial \Phi_1}{\partial r} - \omega^2 \Phi_1 = \kappa \omega_0^2 R_* \frac{\partial \Phi_2}{\partial r} - \kappa \omega^2 \Phi_2. \quad (8)$$

Continuity of V_r gives another boundary condition at the interface

$$\frac{\partial \Phi_1}{\partial r} = \frac{\partial \Phi_2}{\partial r}. \quad (9)$$

Eq. (7) and the boundary conditions (8), (9) constitute a complete set of equations necessary to determine the normal modes of the system. We expand the velocity potential in terms of spherical harmonics $\Phi = \Phi(r)Y_{lm}(\theta, \phi)$. From (7) the radial component can be written in terms of hypergeometric functions $\Phi_1 = C_1 r^l F(\alpha, \beta, l + 3/2, r^2/R_1^2)$, $\Phi_2 = C_2 r^l F(\alpha, \beta, 1, 1 - r^2/R_2^2)$, where $\alpha + \beta = l + 3/2$, $\alpha\beta = (l - \omega^2/\omega_0^2)/2$. From matching boundary conditions, we finally obtain the eigenvalue equation for the normal mode frequencies

$$\frac{\omega^2}{\omega_0^2} = (1 - \kappa) \frac{[l(l + 3/2) + (l - \omega^2/\omega_0^2)\lambda x s_1(\omega, x)] [l - (l - \omega^2/\omega_0^2)x s_2(\omega, x)]}{[l(l + 3/2)(1 - \kappa) - x(l - \omega^2/\omega_0^2)(\kappa\lambda s_1(\omega, x) + (l + 3/2)s_2(\omega, x))]}, \quad (10)$$

where $s_1(\omega, x) = F(\alpha + 1, \beta + 1, l + 5/2, \lambda x)/F(\alpha, \beta, l + 3/2, \lambda x)$, $s_2(\omega, x) = F(\alpha + 1, \beta + 1, 2, 1 - x)/F(\alpha, \beta, 1, 1 - x)$, $x = R_*^2/R_2^2$.

One special solutions of Eq. (10) is $\omega^2 = l\omega_0^2$, which coincide with those for the one component condensate [18]. For this solution the components oscillate in-phase and $\Phi_1 = \kappa\Phi_2 \propto r^l Y_{lm}(\theta, \phi)$. Another special exact solution is $\omega^2 = 5\omega_0^2$ with $\Phi_1 \propto 1 - 5r^2/3R_1^2$, $\Phi_2 \propto \lambda(1 - 5r^2/3R_2^2)$. For this solution the components oscillate out-of-phase if $\sqrt{3/5}R_1 < R_* < \sqrt{3/5}R_2$ and in-phase otherwise. In general we have solved Eq. (10) numerically and found the normal mode frequencies ω of the two component condensate as a function of the parameter $\kappa = \sqrt{a_{11}/a_{22}}$ for a fixed ratio R_*/R_2 . The ratio R_*/R_2 can be directly measured experimentally. Fig. 1 shows the low frequency modes that become imaginary at $\kappa > 1$. These modes are peculiar for the two component systems and are analogous to the waves at the interphase between two layers of immiscible fluids under gravity [19]. For this system, when the top layer becomes denser, the gravitational energy becomes higher and the system becomes unstable. In a similar manner as soon as κ becomes greater than 1, our system becomes unstable.

In the region $|1 - \kappa| \ll 1$ the mode frequencies are small: $|\omega| \ll \omega_0$. We obtain

$$\omega^2 \approx \omega_0^2(1 - \kappa)f(l, x), \quad (11)$$

where

$$f(l, x) = \frac{l(l + 3/2 + xs_1(0, x))(xs_2(0, x) - 1)}{x[s_1(0, x) + (l + 3/2)s_2(0, x)]} > 0.$$

Eq. (11) describes the behavior of the low frequency modes in the region close to the point of instability $\kappa = 1$. In this region $\omega \propto \sqrt{1 - \kappa}$ and becomes imaginary when $\kappa > 1$. We next address the correction of this equation due to the finite overlap of the wave function and the surface tension.

In the TF limit the interface tension results in small corrections of the order of ξ/R_2 to the normal mode frequencies. However, for the low frequency modes in the vicinity $\kappa \approx 1$ the effect of interface tension is substantial because the mode frequencies themselves are close to zero. The interface tension σ modifies the boundary condition for the pressure so that the pressure difference at the interface is equal to the surface pressure $P_1 - P_2 = \sigma(1/r_1 + 1/r_2)$, where r_1, r_2 are the principle radii of curvature. As a result, the ratio of densities at the interphase is

$$\frac{n_2}{n_1} = \sqrt{\kappa^2 - \frac{4\sigma}{G_{22}n_1^2R_*}} = \kappa_{\text{eff}}.$$

The interface tension is given by [20]

$$\sigma = \frac{4}{\sqrt{3}} \sqrt{(\xi_1^2 + \xi_2^2) [a_{12}/\sqrt{a_{11}a_{22}} - 1]} P, \quad (12)$$

where ξ_i represents the single condensate coherence length $\xi_i = \hbar/\sqrt{2m_i G_{ii} n_i}$, the pressure $P \approx G_{ii} n_i^2/2$ and the condensate densities n_i are estimated near the interface. Using the modified boundary condition Eq. (11) is changed to

$$\omega^2 \approx \omega_0^2 \left(1 - \frac{3\sigma}{2R_*P} + \frac{\sigma(l-1)(l+2)}{mn_1\omega_0^2R_*^3} - \kappa_{\text{eff}} \right) f. \quad (13)$$

The interface tension shifts the frequencies of the lowest modes and changes the stability region. For $l = 0$ the inner droplet moves as a whole without changing its shape. However, the displacement of the droplet into the less dense region decreases the interface energy which is proportional to $n^{3/2}$. This is the origin for the contribution $-3\sigma/R_*P$ to the mode frequency. As κ increases the mode with $l = 1$ becomes imaginary first. This determines the system's stability limit. The two component condensate is locally unstable when

$$\frac{a_{11}}{a_{22}} > 1 - \frac{\sigma}{R_*P} = 1 - \frac{4\sqrt{6}\xi}{3R_*} (a_{12}/\sqrt{a_{11}a_{22}} - 1)^{1/2}. \quad (14)$$

We next turn our attention to the calculation of the global stability condition. In the asymmetric phase, we have component one on the right and component two on the left (Fig. 2). In the TF approximation, the density distribution is again given by Eqs. (3), (4). The position of the interphase boundary between them is now different. We determine the global stability condition by equating the energy of the symmetric and the asymmetric phases. The calculation is similar to our previous work [16]. In the limit $N_1 \ll N_2$ we find a simple expression for the line of global instability:

$$\frac{a_{11}}{a_{22}} = 1 - 4 \left(\frac{\sqrt{6}\xi}{R_*} \right)^{1/2} (a_{12}/\sqrt{a_{11}a_{22}} - 1)^{1/4}. \quad (15)$$

In general, the calculation can only be carried out numerically. In Fig. 3 we plot the phase diagram that shows different stability regions of two component condensates. In our estimates we take $\xi/R_* = 0.01$. When $a_{12} < \sqrt{a_{11}a_{22}}$ the homogeneous binary mixture is a stable state. Otherwise the two components are phase separated. In the phase separated region for small ratios of a_{11}/a_{22} the state (1, 2) with the first component inside and the second outside is the only stable configuration. As the ratio a_{11}/a_{22} increases this configuration becomes globally unstable when we cross the left (solid) curve. However, the system is locally stable since the configuration corresponds to a local minima of energy. As a_{11}/a_{22} is further increased, we cross the line of local stability (second solid line) and the (1, 2) state becomes unstable towards transforming into a new stable asymmetric state. In between the two solid lines, the system may tunnel quantum-mechanically from the (1, 2) state to the asymmetric phase. A possible scenario is via quantum nucleation. How this takes place in detail is beyond the scope of the present paper. Eventually the asymmetric phase becomes the (2, 1) state as κ is further increased. If initially the system is prepared in the (2, 1) state then as the ratio a_{11}/a_{22} is decreased this configuration first becomes globally unstable when we cross the right dotted line and locally unstable when a_{11}/a_{22} is close enough to 1.

In summary, we have elucidated in detail a new symmetric-asymmetric transition in mixtures of BEC's. To simplify the numerical details, we have presented our results assuming the trapping frequencies of the two components are the same. Experimentally, the transition can be observed by either changing the interaction strengths or the ratio of the trapping frequencies.

This work was supported by NASA, Grant No. NAG8-1427.

- [1] T.-L. Ho, and V. B. Shenoy, Phys. Rev. Lett. **77**, 3276 (1996).
- [2] B. D. Esry *et al.*, Phys. Rev. Lett. **78**, 3594 (1997).
- [3] H. Pu, and N. P. Bigelow, Phys. Rev. Lett. **80**, 1130 (1998).
- [4] P. Öhberg, and S. Stenholm, Phys. Rev. A. **57**, 1272 (1998).
- [5] S. T. Chui and P. Ao, Phys. Rev. A, **59**, 1473, (1999).
- [6] S. T. Chui, P. Ao, and B. Tanatar, J. Phys. Soc. Jpn., **15**, 142, 1999.
- [7] P. Ao, and S. T. Chui, Phys. Rev. A **58**, 4836 (1998).
- [8] C. J. Myatt *et al.*, Phys. Rev. Lett. **78**, 586 (1997).
- [9] D. S. Hall *et al.*, Phys. Rev. Lett. **81**, 1539 (1998).
- [10] J. Stenger *et al.*, Nature (London) **396**, 345 (1998).
- [11] H.-J. Miesner *et al.*, Phys. Rev. Lett., **82**, 2228, (1999).
- [12] D. M. Stamper-Kurn *et al.*, Phys. Rev. Lett., **83**, 661, (1999).
- [13] M. R. Matthews *et al.*, Phys. Rev. Lett. **81**, 243 (1998).
- [14] D. S. Hall *et al.*, Phys. Rev. Lett., **81**, 1543, (1998).
- [15] M. R. Matthews *et al.*, Phys. Rev. Lett., **83**, 2498, (1999).
- [16] S. T. Chui, V. N. Ryzhov, and E. E. Tareyeva, Pis'm. Zh. Éksp. Teor. Fiz. **75**, 279 (2002) [JETP Letters **75**, 233 (2002)].
- [17] A. L. Fetter, Phys. Rev. A **53**, 4245 (1996).
- [18] S. Stringari, Phys. Rev. Lett. **77**, 2360 (1996).
- [19] L. D. Landau, and E. M. Lifshits, *Hydrodynamics*, Moscow, Nauka, (1988), Sec. 12.
- [20] E. Timmermans, Phys. Rev. Lett. **81**, 5718 (1998).

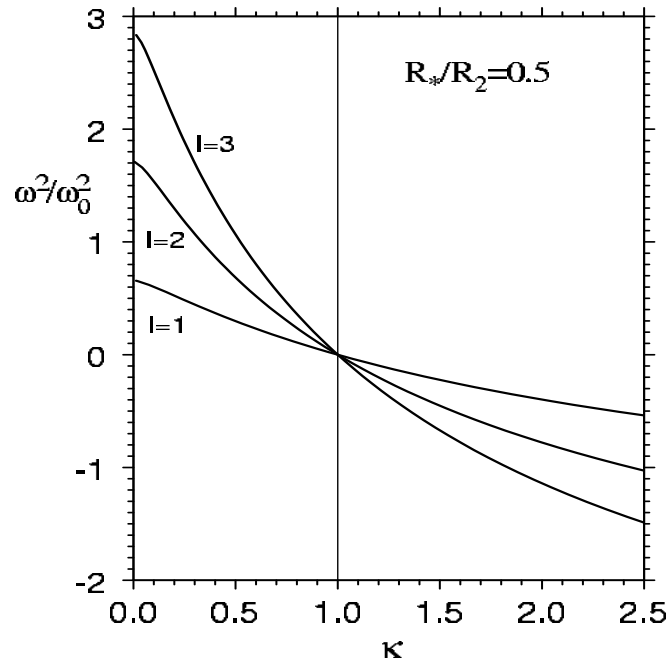


Fig. 1. Low frequency modes as a function of $\kappa = \sqrt{a_{11}/a_{22}}$ for different $l = 1, 2, 3$. The position of the interface is $R_* = R_2/2$. Frequencies become imaginary at $\kappa > 1$.

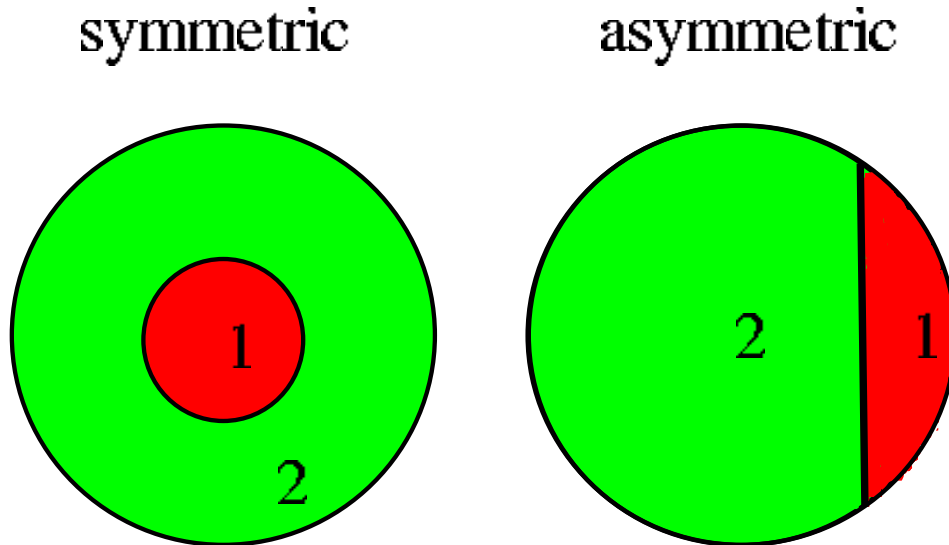


Fig. 2. Symmetric and Asymmetric phases of two component BECs

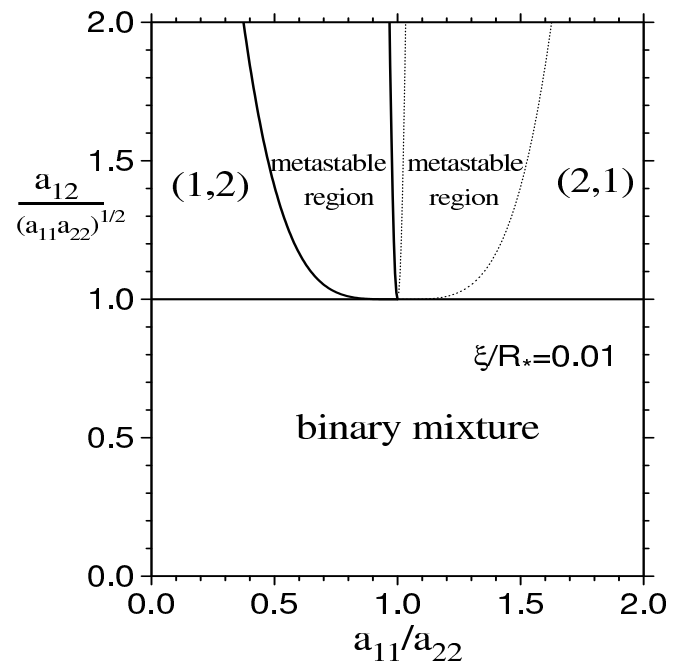


Fig. 3. Phase diagram of the two component condensate in coordinates displaying relative interaction strength between bosons.